Hindawi
Advances in Materials Science and Engineering
Volume 2019, Article ID 7573635, 8 pages
https://doi.org/10.1155/2019/7573635

Research Article

Effects of Aging on the Tensile Properties of Polyethylene Fiber-Reinforced Alkali-Activated Slag-Based Composite

Jeong-Il Choi,[1] Se-Eon Park,[2] Su-Tae Kang,[3] and Bang Yeon Lee[4]

[1]*Graduate Student, School of Architecture, Chonnam National University, 77 Yongbong-ro, Buk-gu, Gwangju 61186, Republic of Korea*
[2]*Researcher, School of Architecture, Chonnam National University, 77 Yongbong-ro, Buk-gu, Gwangju 61186, Republic of Korea*
[3]*Associate Professor, Department of Civil Engineering, Daegu University, 201 Daegudae-ro, Jillyang, Gyeongsan, Gyeongbuk 38453, Republic of Korea*
[4]*Professor, School of Architecture, Chonnam National University, 77 Yongbong-ro, Buk-gu, Gwangju 61186, Republic of Korea*

Correspondence should be addressed to Bang Yeon Lee; bylee@jnu.ac.kr

Received 18 May 2019; Accepted 7 August 2019; Published 27 August 2019

Academic Editor: Paweł Kłosowski

Information on the effect of age on the tensile behavior of fiber-reinforced alkali-activated slag-based composite is fairly limited. Therefore, the purpose of this study is to experimentally investigate the effect of age on the compressive strength and tensile properties of the fiber-reinforced alkali-activated slag-based composite. A binder including slag and alkali activators, chemical admixtures, and a reinforcing fiber were selected, and the mixture proportion was determined to make a fiber-reinforced alkali-activated slag-based composite with high ductility. Compressive strength and tensile strength tests were performed, and values were measured at 3, 5, 7, 14, 28, and 90 days. Test results showed that the compressive strength increased as the age increased. Although the first-cracking strength increased like the compressive strength, the increases of tensile strength and tensile strain capacity were not significant compared with those of compressive strength and first-cracking strength.

1. Introduction

More concrete is produced and consumed than any other synthetic materials on earth, and the amount of concrete used as a construction material is nearly twice that of all other industrial construction materials combined, including wood, iron, plastic, and aluminum [1]. This is attributed to the fact that concrete has high compressive strength and high durability; it is also inexpensive compared to other construction materials. Concrete, however, exhibits relatively low tensile strength—approximately 10% of its compressive strength—and inherently brittle behavior [2]. To overcome these mechanical limitations, fiber-reinforced concrete incorporating discrete short fibers has been developed [3–6]. Recently, a highly ductile fiber-reinforced cementitious composite has also been developed; this material is characterized by high ductility and strain-hardening behaviors [7]. Another problem of concrete is the large amount of carbon dioxide emitted during its manufacture [8]. It has been reported that the cement industry emits approximately 5% of total human-produced carbon dioxide [9, 10].

Many researchers have investigated methods to reduce the amount of cement used or even to develop cement-free concrete utilizing pozzolanic and latent hydraulic materials [11–16]. Recently, in an effort to simultaneously improve both the mechanical properties and the environmental aspect of concrete, studies have been conducted on high-ductility cement-free composites using alkali-activated binders and synthetic fibers. Lee et al. demonstrated the feasibility of using the alkali-activated slag binder and polyvinyl-alcohol fibers to produce a highly ductile cement-free composite [17]. This composite exhibited a tensile ductility of over 4%, while its compressive strength was

similar to that of typical concrete. Ohno and Li used the alkali-activated fly ash binder and polyvinyl-alcohol fibers to develop a composite with mechanical properties similar to those of a highly ductile alkali-activated slag-based composite [18]. Choi et al. used alkali-activated slag binders and polyethylene (PE) fibers to manufacture an ultrahigh-performance composite with a compressive strength of 55 MPa, tensile strength of 13 MPa, and tensile strain capacity as high as 7.5% [19]. Both highly ductile cement-based composites and highly ductile cement-free composites are hardened by the reaction between binders and water, and thus, their mechanical properties can vary depending on curing age. As in typical concrete, the strength of a highly ductile cement-based composite is known to increase with time; however, it has been reported that its tensile strain capacity behaves in a different manner.

Figure 1 shows the tensile strain capacity of the highly ductile cement-based fiber-reinforced composite over time. Previous studies have shown that ductility increases until a certain age and decreases later until the 28-day age, after which it starts to converge [20, 21]. However, to the best of the authors' knowledge, information concerning the effect of age on the tensile behavior of the alkali-activated slag-based composite is fairly limited. Therefore, the present study aims to experimentally investigate the effect of age on the compressive strength and tensile properties of the fiber-reinforced alkali-activated slag-based composite.

2. Materials and Methods

2.1. Materials and Mixture Proportion. The materials and mixture proportions of the fiber-reinforced alkali-activated slag-based composite investigated in this study are listed in Table 1. Ground-granulated blast furnace slag (GGBS) was used as a source material, and calcium hydroxide and sodium sulfate were used as alkali activators. Slag powder of Type III with the fineness value of 4.320 cm^2/g, as defined in KS F 2563, was applied, and its density was 2.92 cm^3/g. Its chemical composition was investigated using X-ray fluorescence (XRF) analysis, whose results are listed in Table 2. To stimulate the latent hydraulic property of the GGBS, powder-type calcium hydroxide and sodium sulfate were added as alkali activators. To ensure the homogeneous distribution of fibers and appropriate fluidity of the mixture, a superplasticizer (SP) was added, and a defoamer was also used to minimize unintended large pores that might form during the manufacturing of test specimens and influence the compressive strength and tensile behavior. The defoamer used in this study was a mixture of surface active agents and mineral substances without silicone. The PE fiber with a high strength up to 2.700 MPa and a high aspect ratio of 1.500 was used as a reinforcing fiber; the physical properties of the fiber are listed in Table 3.

2.2. Specimen Preparation and Curing Method. To manufacture test specimens, powder-type slag and alkali activators were subjected to dry mixing in a planetary mixer for one minute. Subsequently, mixing water was added, and chemical admixtures, including HRWRA and defoamer, were added and mixed for another three minutes. After ensuring that the paste was uniformly mixed and had proper viscosity to uniformly distribute added fibers, fibers were gradually inserted into the paste. After all fibers were added, the mixture was mixed for another four minutes. After mixing was completed, 18 cube specimens with dimensions of 50 mm × 50 mm × 50 mm were manufactured for compressive strength tests, i.e., three specimens for each age condition: 3-day, 5-day, 7-day, 14-day, 28-day, and 90-day ages. For the evaluation of tensile behavior, 24 test specimens were produced, i.e., four for each age condition. The dimensions of the specimens followed the recommendations of the Japan Society of Civil Engineers (JSCE) [22]. The gauge length of specimens was 80 mm, and the dimensions of the cross section within the gauge length were uniform (13 mm × 30 mm). These manufactured specimens were cured at (23 ± 3)°C and a relative humidity of (60 ± 5)% for two days before being demolded. The demolded specimens were then cured under water in a curing container at a temperature of (23 ± 3)°C for every testing day.

2.3. Test Methods. Density was measured to assess the effect of pores on strength depending on the manufacturing process or curing age. This was calculated by measuring the weight of specimens both in water and in air. Compressive strength was measured in accordance with ASTM C109-07 [23], and the uniaxial tensile test and test setup were performed in accordance with JSCE recommendations [22]. An electric universal testing machine with a maximum capacity of 20 kN was used, and the test was carried out under displacement control at a loading rate of 0.1 mm/min. Load was measured using a load cell attached to the machine; for displacement measurement, jigs were installed on the upper and bottom sides of the specimen, where its cross section (30 mm × 13 mm) remained constant, and two linear variable differential transducers (LVDTs) were also attached there [24, 25]. The deformation of specimens occurring within the gauge length of 80 mm was measured by LVDTs, and the resulting two displacement measurements were averaged to calculate the average strain of each specimen. The stress was calculated by dividing the measured load obtained from the load cell by the cross-sectional area of the specimen (390 mm^2), and the strain was calculated by dividing the measured deformation by 80 mm.

3. Results and Discussion

3.1. Density and Compressive Strength. The measured density and compressive strength of the composite are listed in Table 4. Based on the density of each component and the mixture proportion, the theoretical density was found to be 2.06 g/cm^3. When this value was compared to the density data measured at each age, the difference was within 0.5% for all curing ages. This result suggests that unintended large pores were not generated in the specimens that were produced in accordance with the manufacturing procedures

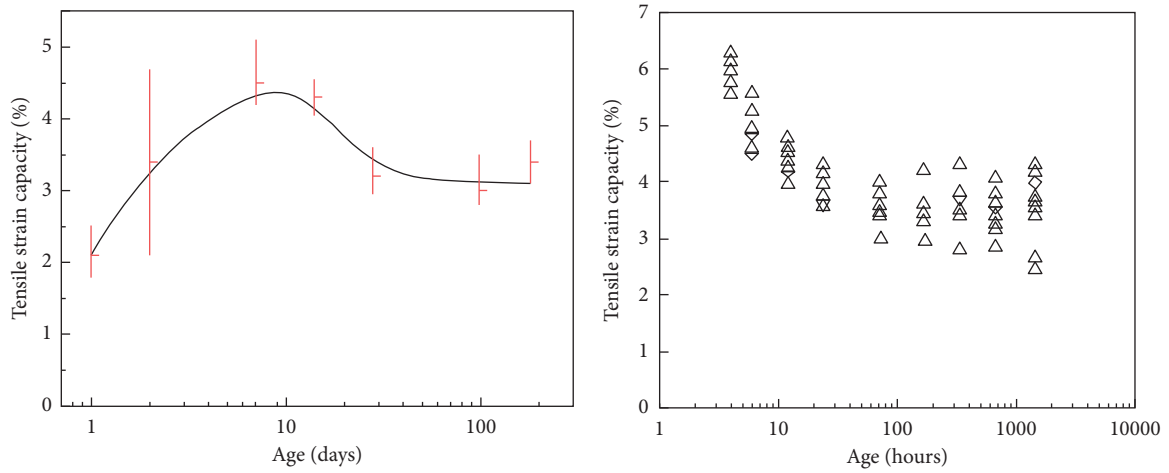

Figure 1: Tensile strain capacity of the highly ductile cement-based fiber-reinforced composite with time: (a) Wang and Li [21]; (b) Li and Li [20].

Table 1: Mixture proportions.

Mixture	Binder			Water	SP	Defoamer	Fiber (vol.%)
	GGBS	$Ca(OH)_2$	Na_2SO_4				
PE-AAS	0.895	0.075	0.030	0.25	0.014	0.001	1.75

Note. Weight ratios of binder weight except fiber.

Table 2: Chemical compositions of GGBS (%).

CaO	SiO_2	Al_2O_3	MgO	SO_3	TiO_2	K_2O	Fe_2O_3	MnO	Na_2O	Others
40.4	30.6	13.8	8.0	4.0	0.9	0.5	0.5	0.5	0.4	0.4

Table 3: Properties of fibers.

Type of fiber	Diameter (μm)	Length (mm)	Tensile strength (MPa)	Density (g/cm^3)	Elastic modulus (GPa)
PE	12	18	2.700	0.97	88

Table 4: Density and compressive strength.

Age (days)	Theoretical density (g/cm^3)	Measured density (g/cm^3)	Compressive strength (MPa)
3	2.06	2.07 ± 0.01	34.0 ± 1.6
5	2.06	2.06 ± 0.01	37.4 ± 0.8
7	2.06	2.07 ± 0.01	38.9 ± 1.0
14	2.06	2.06 ± 0.01	43.6 ± 1.4
28	2.06	2.07 ± 0.01	47.8 ± 1.5
90	2.06	2.06 ± 0.01	53.4 ± 1.0

used in the present study; thus, it was possible to neglect the effects of such pores on the strength.

As expected, compressive strength tended to gradually increase with curing age. The strength development of the composite was compared with models suggested by *fib* Model Code 2010 [26] and ACI Committee 209 [27] (Figure 2). The strength class of cement of 42.5 N was selected from the *fib* model because the compressive strength of the composite was 47.8 MPa. Therefore, 0.25 was selected as the coefficient(s). In the ACI model, α and β were 4.0 and 0.85, respectively. As can be seen in Figure 2, until 28 days, the composite showed faster strength development than was found when using the *fib* and ACI models, while the sample showed similar strength development thereafter. This indicates the potential that the composite investigated in this study may show convergence of tensile behavior faster than

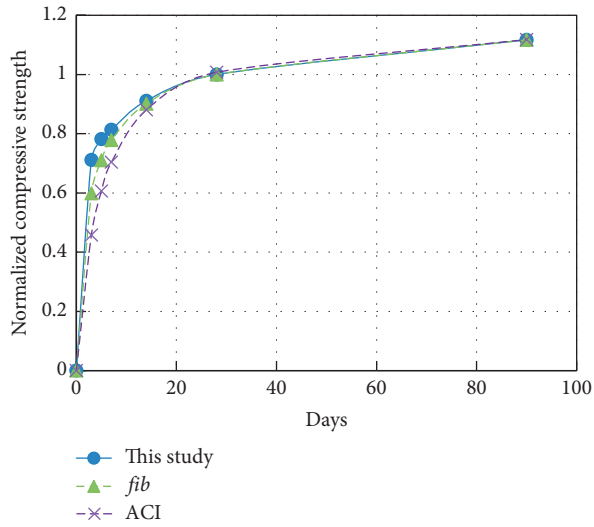

Figure 2: Normalized compressive strength of the fiber-reinforced alkali-activated slag-based composite with time.

that of the highly ductile cement-based fiber-reinforced composite.

3.2. Tensile Behavior. Figure 3 shows the tensile stress and strain curves at each age for the composite investigated in this study. In contrast to normal concrete or fiber-reinforced concrete, which exhibits strain softening after the occurrence of an initial crack, the composite manufactured in this study showed multiple-cracking, strain-hardening, and ductile behaviors. For all ages, the occurrence of cracks led to sudden stress drop because load was applied under displacement control. Each time a crack formed, the width of the crack instantaneously increased, thereby relaxing the stress on other parts of the specimen and thus resulting in a decrease in load. Therefore, the number of load or stress drop events corresponded to the number of cracks.

The reason why cracks occur in a consecutive manner is that the cracking strength of a specimen varies depending on crack position within the specimen. Meanwhile, strain hardening occurs when the fiber-bridging stress exceeds the cracking strength of the composite, and this continues as long as this condition is satisfied. This is called the strength condition, and it is quantitatively evaluated using the stress performance index, which is calculated according to the ratio of the tensile strength to the first-cracking strength [28]. For multiple cracking and strain hardening to occur, aside from the above strength condition, one energy condition should also be satisfied, as follows: the amount of energy needed for a crack width to increase must exceed the amount of energy needed for the crack to propagate, thereby giving rise to steady-state cracks having constant width [29]. In cases in which the maximum fiber-bridging stress is less than the cracking strength, or the energy condition is not fully satisfied in a specific part of the specimen, the width of cracks in the part will continue to increase, thereby causing localized fractures and further strain softening.

The tensile behavior of a material can be quantitatively represented by the first-cracking strength (f_{cr}), tensile strength (f_t), and tensile strain capacity. Table 5 lists the first-cracking strength, tensile strength, tensile strain capacity, and toughness of the composite at each age. As can be seen in Figure 3, the first-cracking strength refers to the stress measured at the part where a load reduction was first observed in the tensile stress and strain curves. The tensile strength represents the maximum fiber-bridging stress. The tensile strain capacity refers to the tensile strain corresponding to the tensile strength. The toughness refers to the area below the stress and strain curve, which represents the capacity of the material to absorb energy before its fracture. In this study, toughness was calculated while considering the part of each graph where strain-hardening behavior was observed.

The first-cracking strength tended to gradually increase with curing age, as was shown in the compressive strength analysis. This is because the cracking strength of a specimen is determined by the properties of its matrix, which are generally proportional to its compressive strength. In Figure 4, the ratio of the first-cracking strength to the compressive strength is plotted. Although this ratio slightly decreased with curing age, the difference was not significant and the values were about 10%. This result is similar to that for normal concrete [2].

The tensile strength continued to increase until the 7-day age, decreased by 4.7% at the 14-day age, and started to increase again later on. After the 7-day age, it alternately decreased and increased; however, the corresponding coefficient of variation was within the range of 8%–15%. Ratios of the tensile strengths to the corresponding compressive strengths are shown in Figure 4. Here, all values were over 20% at all ages, and it was found that the ratio gradually converged after the 14-day age. For normal concrete, this ratio is as low as 10%. This is why, in the ultimate strength design method, it is assumed that the tensile strength of concrete is zero. The composite investigated in the present study, however, showed a relatively high ratio of tensile strength to compressive strength, which means that it has the potential to improve the performance of structures or structural members when it is used.

Figure 5 shows the tensile strain capacity of composites with time. The tensile strain capacity of the composite investigated in the present study increased until the 7-day age and decreased later until the 28-day age, after which it started to converge. This observation is similar to the report in the previous study [21]. High-early-strength engineered cementitious composites using rapid-hardening cement showed faster convergence in tensile strain capacity [20]. It should be noted that, for highly ductile cement-based fiber-reinforced composites, i.e., engineered cementitious composites (ECCs), the 90-day tensile strain capacity was 30%~40% lower than the maximum tensile strain capacity, whereas the 90-day tensile strain capacity of the fiber-reinforced alkali-activated slag-based composite was only 4.8% less than its maximum value. These results show that the effect of curing age on the tensile strain capacity is relatively smaller for the composite investigated in the

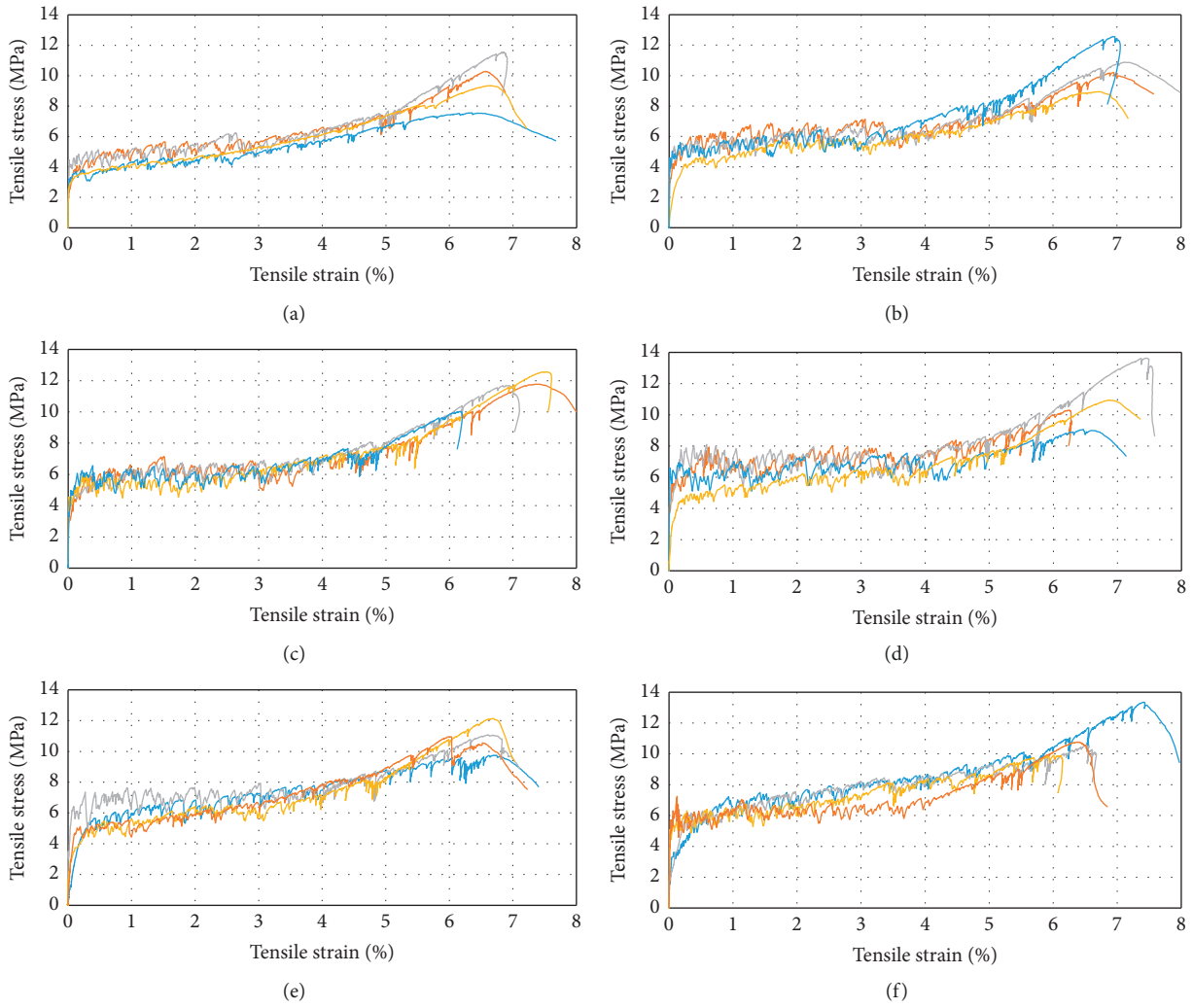

Figure 3: Tensile stress and strain curves: (a) 3 days; (b) 5 days; (c) 7 days; (d) 14 days; (e) 28 days; (f) 90 days.

Table 5: Uniaxial tensile behavior.

Age (days)	First-cracking strength (MPa)	Tensile strength (MPa)	Tensile strain capacity (%)	Toughness (MPa·m/m)	Strength performance index
3	3.65 ± 0.72	9.63 ± 1.40	6.58 ± 0.19	0.44	2.64
5	3.79 ± 0.56	10.70 ± 1.17	7.03 ± 0.10	0.51	2.82
7	3.93 ± 0.57	11.14 ± 0.79	7.07 ± 0.56	0.53	2.83
14	4.43 ± 0.43	10.97 ± 1.67	6.85 ± 0.46	0.53	2.48
28	4.58 ± 0.79	10.98 ± 0.97	6.81 ± 0.04	0.53	2.40
90	4.84 ± 0.91	11.27 ± 1.49	6.73 ± 0.53	0.54	2.33

present study than it is in highly ductile cement-based fiber-reinforced composites [20, 21]. Furthermore, the fiber-reinforced alkali-activated slag-based composite showed approximately two times higher tensile strain capacity than that of highly ductile cement-based fiber-reinforced composites. It was observed that the toughness of the fiber-reinforced alkali-activated slag-based composite increased until the 7-day age and then converged. The composite showed a higher stress performance index exceeding 1 for all ages, which means that the composite satisfied the minimum stress performance index for the multiple-cracking and strain-hardening behaviors.

Figure 6 shows representative crack patterns observed at each curing age in the fiber-reinforced alkali-activated slag-based composite specimens. In all specimens, multiple fine cracks are observed. Also, cracks appear to be more linear with increasing curing age, and this is because the fracture mode of their matrix becomes more brittle.

Table 6 lists the number of cracks, the crack spacing, and the crack width for the fiber-reinforced alkali-activated slag-

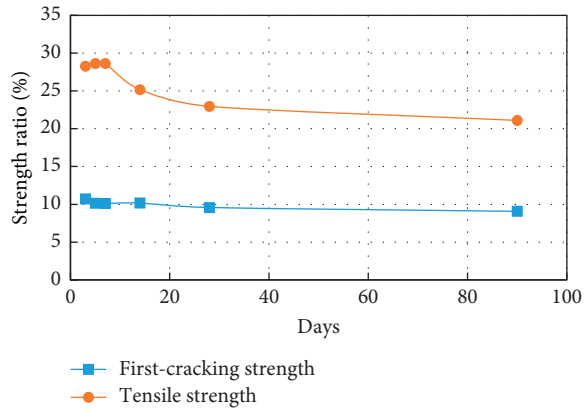

Figure 4: Ratio of the first-cracking strength and the tensile strength to the compressive strength with time.

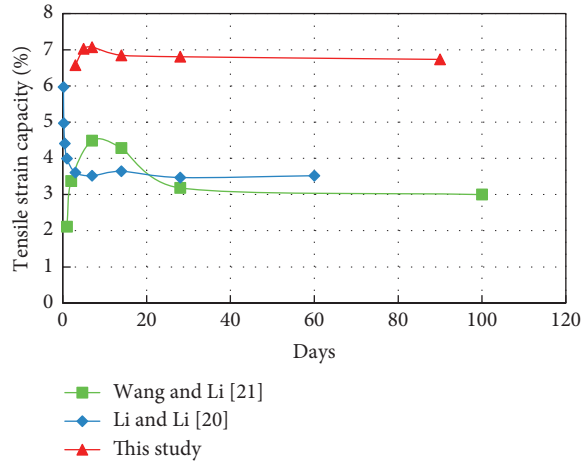

Figure 5: Tensile strain capacity of composites with time.

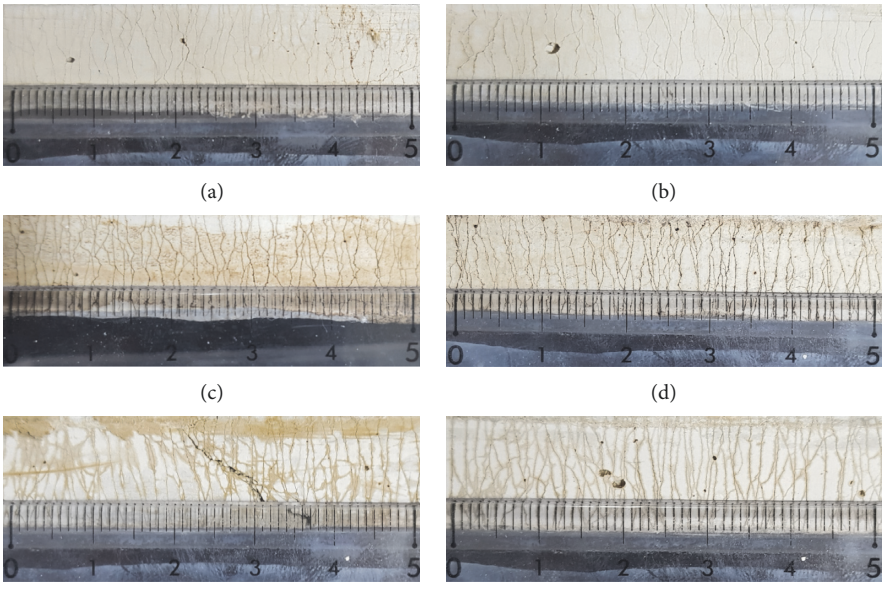

Figure 6: Cracking patterns (unit of numbers: cm): (a) 3 days; (b) 5 days; (c) 7 days; (d) 14 days; (e) 28 days; (f) 90 days.

Table 6: Cracking pattern.

Age (days)	Number of cracks within gauge length (80 mm)	Crack spacing (mm)	Crack width (μm)
3	89.9 ± 11.3	0.90 ± 0.10	60.3 ± 8.2
5	82.1 ± 3.1	0.98 ± 0.04	68.5 ± 2.5
7	90.9 ± 7.0	0.89 ± 0.07	62.8 ± 8.3
14	103.5 ± 2.3	0.76 ± 0.02	51.4 ± 2.7
28	101.7 ± 7.9	0.79 ± 0.06	53.9 ± 4.0
90	99.8 ± 7.1	0.81 ± 0.06	50.5 ± 4.5

based composite specimens. Here, the number of cracks refers to the average number of cracks formed within a gauge length of 80 mm where deformation and strain were measured. The number of cracks formed on both sides of each specimen was manually counted after the tensile test. Notably, this number of cracks is identical to that from the corresponding tensile strength analysis because no more cracks were created after the tensile stress reached the tensile strength. The crack spacing was calculated by dividing the number of cracks by the gauge length. The crack width was determined by dividing the measured deformation within the gauge length when the tensile strength was reached by the number of cracks, under the assumption that the entire deformation within the gauge length is identical to the summation of all crack openings. This is because any crack opening is much larger than the elastic deformation of the uncracked matrix.

It was observed that there were variations in the number of cracks, in the crack spacing, and in the crack width of the composite with time until the 14-day age; then, the number of cracks, the crack spacing, and the crack width of the composite converged. For all ages, saturated cracking patterns were observed. The number of cracks was over 80 within the gauge length of 80 mm, which means that the crack spacing is smaller than 1 mm. The crack width converged to a value below 60 μm after the 14-day age. A previous study reported that the water permeability coefficient of the cementitious composite with cracks whose width is below 60 μm is on the same order of magnitude as that of an uncracked cementitious composite [30]. From these observations, it can be expected that the fiber-reinforced alkali-activated slag-based composite investigated in this study has high durability in terms of water permeability and water tightness.

4. Conclusion

This study experimentally investigated the effect of age on the compressive strength and tensile properties of a PE fiber-reinforced alkali-activated slag-based composite with high tensile ductility. A series of experimental tests were carried out to investigate the mechanical properties of the composite over time. The following conclusions can be drawn from the current experimental results:

(1) The compressive strength of the fiber-reinforced alkali-activated slag-based composite investigated in this study tended to gradually increase with curing age. However, the development rate of the compressive strength of the composite was faster than that predicted by *fib* and ACI models. The ratio of the first-cracking strength to the compressive strength was approximately 10% regardless of age.

(2) The tensile strength and toughness of the fiber-reinforced alkali-activated slag-based composite increased until the 7-day age and then converged. On the contrary, the tensile strain capacity of the composite tended to increase until the 7-day age and decreased later until the 28-day age, after which it started to converge. It was shown that the effect of age was relatively smaller for the composite investigated in this study than for highly ductile cement-based fiber-reinforced composites.

(3) The number of cracks, the crack spacing, and the crack width showed a relatively smaller variation and then converged after the 14-day age. Overall, in terms of tensile behavior, when compared to the cement-based composite, the composite investigated in this study showed a smaller variance, and its tensile behavior tended to converge after the 14-day age.

Data Availability

The data used to support the findings of this study are available from the corresponding author upon request.

Conflicts of Interest

The authors declare that they have no conflicts of interest.

Acknowledgments

This research was supported a grant (19SCIP-B103706-05) from Construction Technology Research Program funded by the Ministry of Land, Infrastructure and Transport of the Korean government and also supported by a grant (19CTAP-C151882-01) from Technology Advancement Research Program funded by the Ministry of Land, Infrastructure and Transport of the Korean government.

References

[1] H. Van Damme, "Concrete material science: past, present, and future innovations," *Cement and Concrete Research*, vol. 112, pp. 5–24, 2018.

[2] S. Mindess, J. F. Young, and D. Darwin, *Concrete*, Pearson Education, Inc., Upper Saddle River, NJ, USA, 2nd edition, 2002.

[3] ACI Committee 544, *544.1R-96: Report on Fiber Reinforced Concrete*, American Concrete Institute, Farmington, MI, USA, 1996.

[4] P. Smarzewski and D. Barnat-Hunek, "Effect of fiber hybridization on durability related properties of ultra-high performance concrete," *International Journal of Concrete Structures and Materials*, vol. 11, no. 195, pp. 315–325, 2017.

[5] L. Xu, B. Li, X. Ding et al., "Experimental investigation on damage behavior of polypropylene fiber reinforced concrete under compression," *International Journal of Concrete Structures and Materials*, vol. 12, no. 68, pp. 1–20, 2018.

[6] J.-M. Yang, D.-Y. Yoo, Y.-C. Kim, and Y.-S. Yoon, "Mechanical properties of steam cured high-strength steel fiber-reinforced concrete with high-volume blast furnace slag," *International Journal of Concrete Structures and Materials*, vol. 11, no. 200, pp. 391–401, 2017.

[7] M. Maalej and V. C. Li, "Flexural/tensile-strength ratio in engineered cementitious composites," *Journal of Materials in Civil Engineering*, vol. 6, no. 4, pp. 513–528, 1994.

[8] A. Imam, V. Kumar, and V. Srivastava, "Empirical predictions for the mechanical properties of quaternary cement concrete," *Journal of Structural Integrity and Maintenance*, vol. 3, no. 3, pp. 183–196, 2018.

[9] V. Malhotra, "Introduction: sustainable development and concrete technology," *Concrete International*, vol. 24, no. 7, p. 22, 2002.

[10] J. S. Damtoft, J. Lukasik, D. Herfort, D. Sorrentino, and E. M. Gartner, "Sustainable development and climate change initiatives," *Cement and Concrete Research*, vol. 38, no. 2, pp. 115–127, 2008.

[11] V. Bílek, L. Kalina, R. Novotný, J. Tkacz, and L. Pařízek, "Some issues of shrinkage-reducing admixtures application in alkali-activated slag systems," *Materials*, vol. 9, no. 6, p. 462, 2016.

[12] L. Chen, Z. Wang, Y. Wang, and J. Feng, "Preparation and properties of alkali activated metakaolin-based geopolymer," *Materials*, vol. 9, no. 9, p. 767, 2016.

[13] J.-W. Lee, Y.-I. Jang, W.-S. Park, and S.-W. Kim, "A study on mechanical properties of porous concrete using cementless binder," *International Journal of Concrete Structures and Materials*, vol. 10, no. 4, pp. 527–537, 2016.

[14] F. Pacheco-Torgal, J. Castro-Gomes, and S. Jalali, "Alkali-activated binders: a review. Part 2. About materials and binders manufacture," *Construction and Building Materials*, vol. 22, no. 7, pp. 1315–1322, 2008.

[15] D. M. Roy, "Alkali-activated cements opportunities and challenges," *Cement and Concrete Research*, vol. 29, no. 2, pp. 249–254, 1999.

[16] C. Shi, D. Roy, and P. Krivenko, *Alkali-Activated Cements and Concretes*, CRC Press, Boca Raton, FL, USA, 2003.

[17] B. Y. Lee, C.-G. Cho, H.-J. Lim, J.-K. Song, K.-H. Yang, and V. C. Li, "Strain hardening fiber reinforced alkali-activated mortar—a feasibility study," *Construction and Building Materials*, vol. 37, pp. 15–20, 2012.

[18] M. Ohno and V. C. Li, "A feasibility study of strain hardening fiber reinforced fly ash-based geopolymer composites," *Construction and Building Materials*, vol. 57, pp. 163–168, 2014.

[19] J.-I. Choi, B. Y. Lee, R. Ranade, V. C. Li, and Y. Lee, "Ultra-high-ductile behavior of a polyethylene fiber-reinforced alkali-activated slag-based composite," *Cement and Concrete Composites*, vol. 70, pp. 153–158, 2016.

[20] M. Li and V. C. Li, "High-early-strength engineered cementitious composites for fast, durable concrete repair-material properties," *ACI Materials Journal*, vol. 108, no. 1, p. 3, 2011.

[21] S. Wang and V. C. Li, "Polyvinyl alcohol fiber reinforced engineered cementitious composites: material design and performances," in *Proceedings of the International RILEM Workshop on HPFRCC in Structural Applications*, pp. 65–73, Honolulu, HI, USA, 2006.

[22] JSCE, "Recommendations for design and construction of high performance fiber reinforced cement composites with multiple fine cracks (HPFRCC)," in *Concrete Engineering Series*, Japan Society of Civil Engineers, Tokyo, Japan, 2008.

[23] ASTM C109/C109M-07, *Standard Test Method for Compressive Strength of Hydraulic Cement Mortars (Using 2-in. Or (50-mm) Cube Specimens)*, American Society for Testing and Materials: ASTM International West, Conshohocken, PA, USA, 2007.

[24] J. H. Hyun, B. Y. Lee, and Y. Y. Kim, "Composite properties and micromechanical analysis of highly ductile cement composite incorporating limestone powder," *Applied Sciences*, vol. 8, no. 2, p. 151, 2018.

[25] S.-T. Kang, K.-S. Lee, J.-I. Choi, Y. Lee, B. Felekoğlu, and B. Y. Lees, "Control of tensile behavior of ultra-high performance concrete through artificial flaws and fiber hybridization," *International Journal of Concrete Structures and Materials*, vol. 10, no. 3, pp. 33–41, 2016.

[26] J. Walraven, "*fib* model code for concrete structures 2010: mastering challenges and encountering new ones," *Structural Concrete*, vol. 14, no. 1, pp. 3–9, 2013.

[27] ACI Committee 209, *Prediction of Creep, Shrinkage, and Temperature Effects in Concrete Structures, ACI 209R-92*, American Concrete Institute, Naples, FL, USA, 1992.

[28] T. Kanda and V. C. Li, "Practical design criteria for saturated pseudo strain hardening behavior in ECC," *Journal of Advanced Concrete Technology*, vol. 4, no. 1, pp. 59–72, 2006.

[29] V. C. Li and H.-C. Wu, "Conditions for pseudo strain-hardening in fiber reinforced brittle matrix composites," *Applied Mechanics Reviews*, vol. 45, no. 8, pp. 390–398, 1992.

[30] M. D. Lepech and V. C. Li, "Water permeability of engineered cementitious composites," *Cement and Concrete Composites*, vol. 31, no. 10, pp. 744–753, 2009.